P8.119 PRELIMINARY INVESTIGATION OF TORNADO WARNING SKILL BY ENVIRONMENT

Alexandra K. Anderson-Frey[1]*, Yvette P. Richardson[1], and Andrew R. Dean[2]
[1]Pennsylvania State University, University Park, PA
[2]NOAA Storm Prediction Center, Norman, OK

1. INTRODUCTION

The production of timely and accurate tornado warnings is extremely important to the safety of our society. In order to provide these warnings, forecasters are faced with the difficult task of synthesizing their best estimate of the storm environment (with tornado likelihood often based on a combination of conceptual models), and storm observations that are necessarily incomplete (e.g., radar velocities that are collected significantly above the ground). Given that there is a greater overall understanding of storm dynamics in certain parts of the environmental parameter space, we would expect the skill of those forecasts to be relatively high. Likewise, in the portions of the parameter space that are less well understood, the added uncertainty should lead to a higher number of missed events as well as false alarms.

In this preliminary study, we examine how tornado warning skill varies in terms of environmental parameters that are associated with severe convection. By determining which parts of the parameter space show lower tornado warning skill [i.e., higher false alarm ratio (FAR) and lower probability of detection (POD)] we can then target the environments in which our understanding fails and further research is warranted.

2. METHODS AND DATA

The information employed in this study originates from two large datasets. The first, obtained from the Storm Prediction Center, contains objective analysis data produced using the Rapid Update Cycle (RUC) model (Bothwell et al. 2002). From these data, we determine the values of environmental parameters corresponding to each tornado warning issued and each tornado report received from 2003-2012. For the warnings, we examined each grid box (resolution is 40 km) that intersected the warning and used the grid box with the highest significant tornado parameter [STP, as defined in Thompson et al. (2003)] as the representative environment for the warning. For the tornado report environments, environmental values from the grid box corresponding to the tornado location were used. [For a discussion of analysis accuracy, the reader is referred to Coniglio (2012).] The second dataset, courtesy of the National Weather Service, contains validation information corresponding to each tornado warning issued, dating back to 1986, as well as the official recording of each tornado event and the corresponding warning (if one was issued). Thompson et al. (2003, 2012) provide additional information on the methodology used to create the SPC database.

In this preliminary work, two parameter spaces are investigated: mixed-layer lifted condensation level (ML LCL) versus 0-1 km shear [measured in terms of the vector shear magnitude (i.e., the magnitude of the vector wind difference between two levels)], and most unstable convective available potential energy (MU CAPE) versus 0-6 km shear. Reports and statistics for each of these parameter spaces are then divided into bins that best represent the variability of the environmental parameters across all events/warnings, following the methodology of Schneider and Dean (2008). The current report covers only the 2003-2007 time period, containing county-based warnings. Later polygon-based warnings will be analyzed in future work.

3. PRELIMINARY RESULTS

Warning skill statistics and reports are plotted for each of the two parameter spaces described in the previous section, spanning data from 2003-2007. In the following discussion, a distinction is made between "total fraction" and "bin fraction". The former refers to the fractional contribution of each bin to the total number across all bins, while the latter indicates the percentage occurrence within each individual bin. For instance, each pixel in a plot of *total* fraction of false alarms represents the number of false alarms within that bin, divided by the total number of false alarms across the entire parameter space. Thus, in a total fraction plot, the sum of all bins must equal one, providing an at-a-glance image that highlights the parts of the parameter space that contribute most to the total number of false alarms. In contrast, each pixel in a plot of *bin* fraction of false alarms represents the number of false alarms within that bin divided by the total number of warnings issued within that bin. In this way, a bin fraction plot tends to highlight the regions of the parameter space that have been most poorly forecast, even if those environments are relatively uncommon. In addition, plots of false alarms (or missed events) include only bins containing at least five warnings (or events).

3.1 *ML LCL and 0-1 km Shear*

Within the supercell regime, the height of the mixed-layer LCL is a recognized discriminator of significant tornado environments, with heights below about 1200m AGL tending to result in a higher probability of significant tornadoes. (Rasmussen and Blanchard 1998; Thompson et al. 2003) Likewise,

Corresponding Author Address:
Alexandra Anderson-Frey, Department of Meteorology, The Pennsylvania State University, University Park, PA 16802; e-mail: aka145@psu.edu.

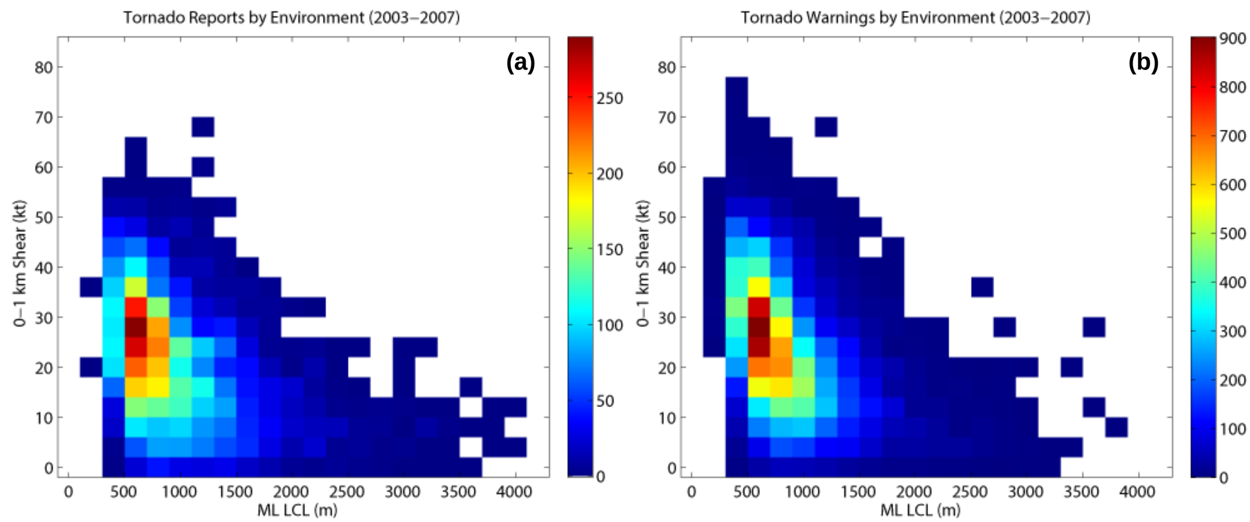

Figure 1: Environmental number plots for mixed-layer LCL (m) and 0-1 km vector shear magnitude (kt). Each bin represents a range of the environmental parameter space. (a) Number of tornado reports for each bin. (b) Number of tornado warnings for each bin. The similarity in shape and density of these distributions suggests a relatively high probability of detection (POD), while the much higher number of warnings compared to the number of reports suggests a relatively high false alarm ratio (FAR).

strong vertical wind shear from 0-1 km has been identified as a characteristic of tornadic supercells, with greater values associated with violent tornadoes (e.g., Markowski et al. 2003; Thompson et al. 2003). In a bin plot of ML LCL and 0-1 km vector shear magnitude, pixels with high values of both would be expected to correspond to environments favorable for significant tornadoes. Figure 1 shows the distribution of tornado reports and tornado warnings, plotted according to the values of ML LCL and 0-1 km vector shear magnitude. The majority of events and warnings occur with between 20-40 kt of vector shear magnitude and with LCL heights between 500-1000 m.

False alarm statistics are then calculated for the ML LCL and 0-1 km shear parameter space, as depicted in Fig. 2. Note the similarity between the total fraction of false alarms in Fig. 2a and the number of tornado warnings in Fig. 1b. The similarity between these two figures demonstrates that the largest total fraction of false alarms occurs in the part of the parameter space where tornado warnings are the most common, as might be expected. Figure 2b, the bin fraction of false alarms, shows that the false alarm ratio (FAR) for each bin is quite similar across the parameter space (with values of around 0.7-0.8), although FAR is somewhat smaller overall for many bins corresponding to ML LCL heights greater than about 1400 m.

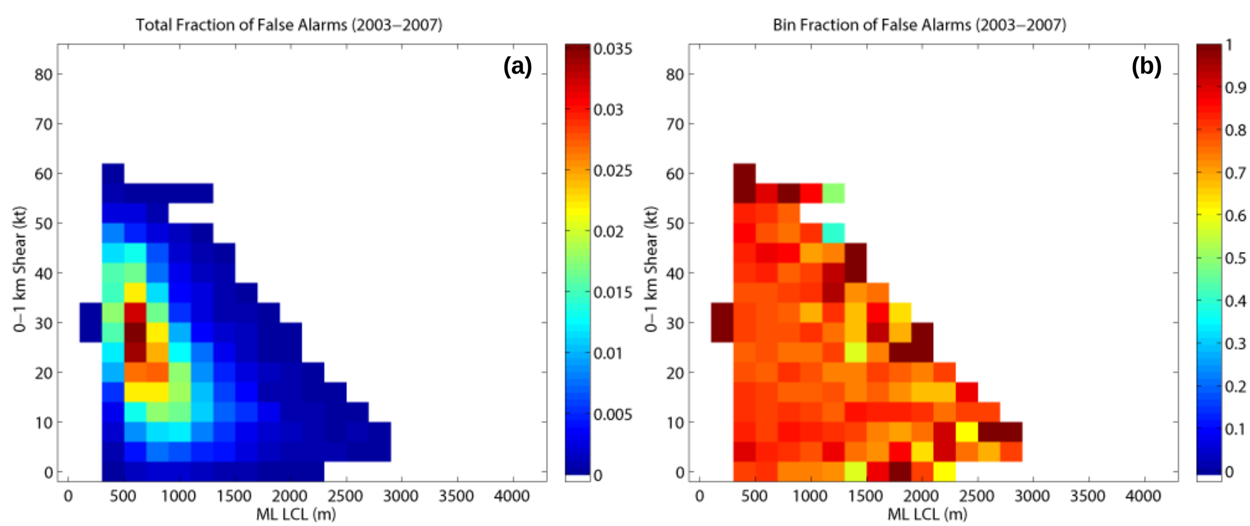

Figure 2: Environmental false alarm plots for mixed-layer LCL (m) and 0-1 km vector shear magnitude (kt). Each bin represents a range of the environmental parameter space, and bins containing fewer than 5 warnings have been removed. (a) Total fraction of false alarms: note the similarity to the total number of warnings in Fig. 1b. (b) Bin fraction of false alarms.

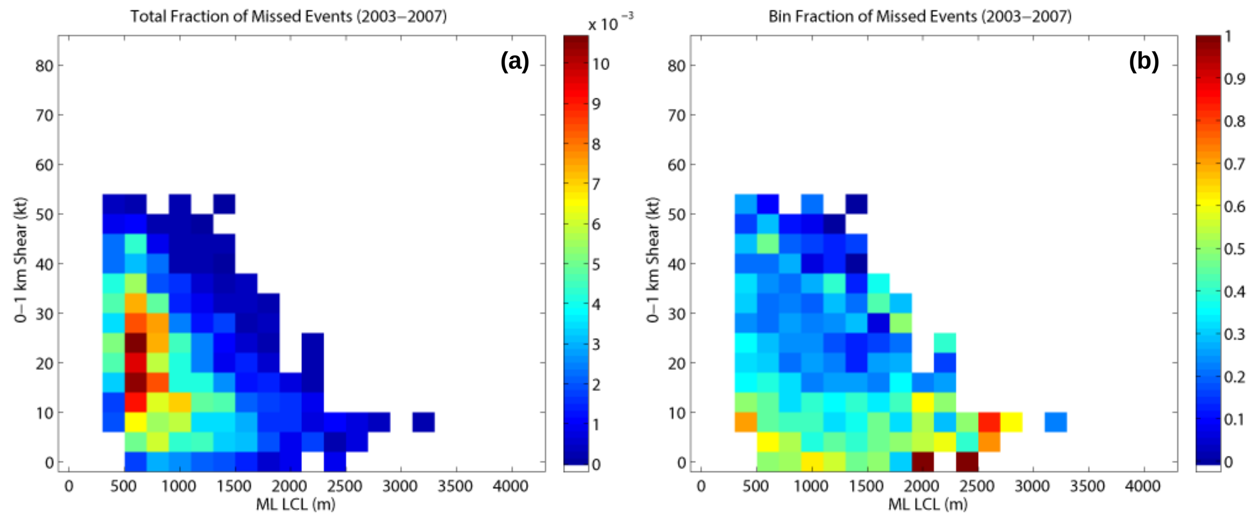

Figure 3: Environmental missed event plots for mixed-layer LCL (m) and 0-1 km vector shear magnitude (kt). Each bin represents a range of the environmental parameter space, and bins containing fewer than 5 events have been removed. (a) Total fraction of missed events: note the similarity to the total number of reports in Fig. 1a. (b) Bin fraction of missed events.

Finally, Fig. 3 depicts the missed event statistics as calculated for the ML LCL and 0-1 km shear parameter space. Once again, the total fraction of missed events in Fig. 3a matches well with the number of tornado reports in Fig. 1a, demonstrating that the largest contribution toward the total number of missed events is coming from the part of the parameter space with the most tornado reports. The bin fraction of missed events in Fig. 3b shows a clear trend in which bins having higher 0-1 km vector shear magnitude (i.e., bins corresponding to conditions more favorable for significant tornadoes) have a lower fraction of missed events. It is worth noting that, below about 15 kt of low-level vector shear magnitude, the bins have a relatively high fraction of missed events, regardless of the height of the ML LCL.

3.2 MU CAPE and 0-6 km Shear

The second parameter space considered in this study features the most unstable CAPE and the 0-6 km vector shear magnitude, the combination of which is generally considered to be a discriminator for severe versus non-severe thunderstorms (e.g., Thompson et al. 2003; Brooks et al. 2003). Figure 4, analogous to Fig. 1 for the first parameter space, depicts the total number of tornado reports by environment, as well as the total number of tornado warnings by environment. The majority of events and warnings occur with 40-60 kt of 0-6 km vector shear magnitude, with MU CAPE values ranging from about 250 to 3000 J/kg.

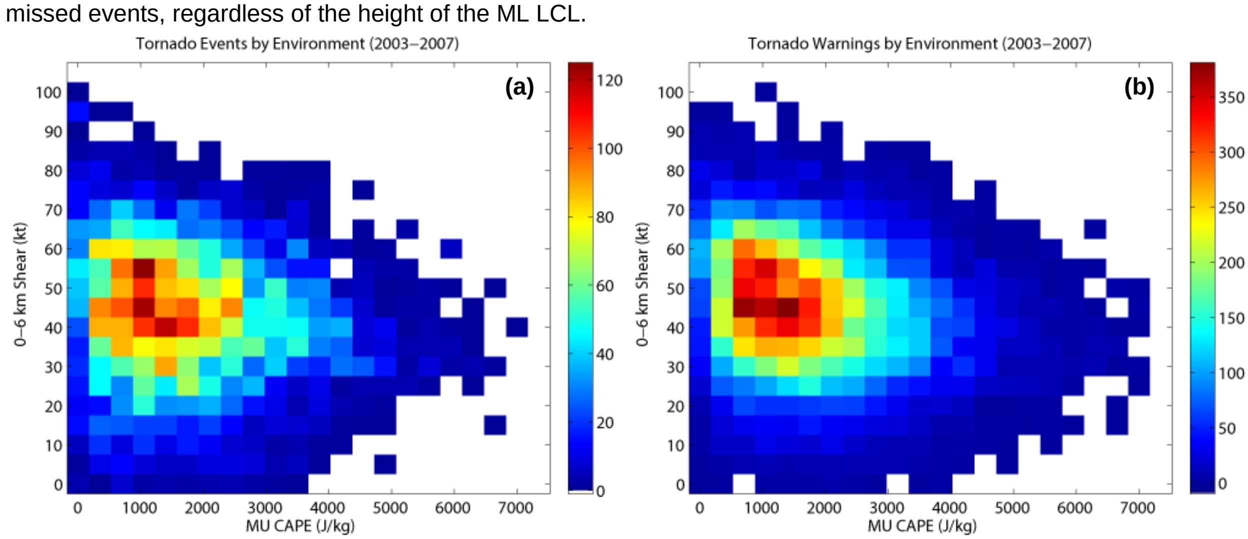

Figure 4: Environmental number plots for most unstable CAPE (J/kg) and 0-6 km vector shear magnitude (kt). Each bin represents a range of the environmental parameter space. (a) Number of tornado reports for each bin. (b) Number of tornado warnings for each bin. The similarity in shape and density of these distributions suggests a relatively high probability of detection (POD), while the much higher number of warnings suggests a relatively high false alarm ratio (FAR).

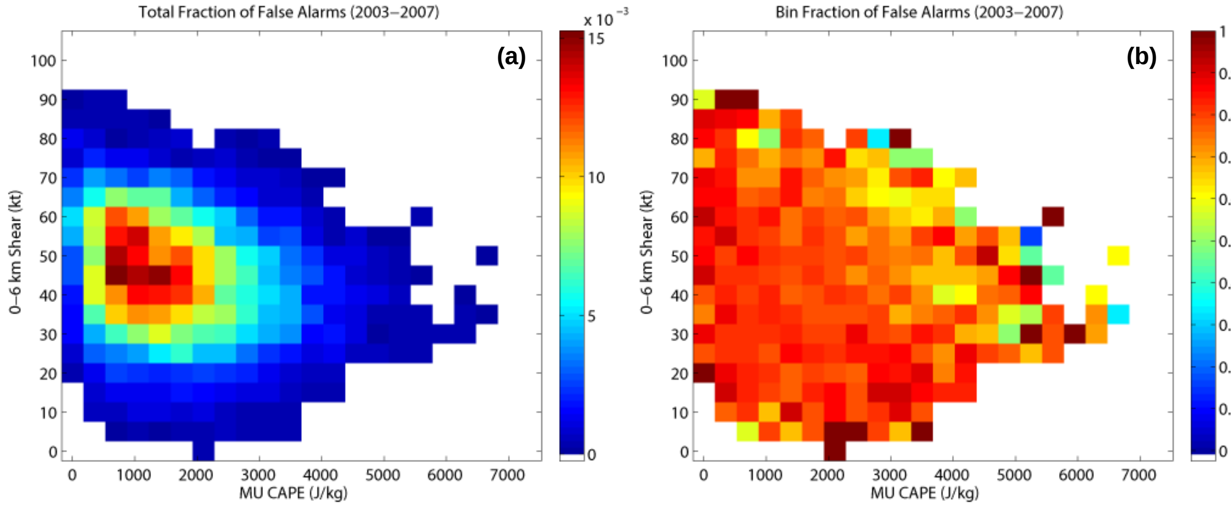

Figure 5: As in Fig. 2, but for most unstable CAPE (J/kg) and 0-6 km vector shear magnitude (kt). Each bin represents a range of the environmental parameter space, and bins containing fewer than 5 warnings have been removed. (a) Total fraction of false alarms: note the similarity to the total number of warnings in Fig. 4b. (b) Bin fraction of false alarms.

Figure 5, analogous to Fig. 2 for the first parameter space, shows the false alarm total and bin fractions for MU CAPE versus 0-6 km vector shear magnitude. As in the first parameter space, the total false alarm fraction plot (Fig. 5a) resembles the number plot for tornado warnings in Fig. 4b; once again, the part of the parameter space containing the majority of warnings is also the one contributing the most false alarms. Figure 5b gives the bin fraction of false alarms, showing that, for relatively high MU CAPE and 0-6 km vector shear magnitude, false alarm rates are somewhat lower than for smaller MU CAPE and vector shear magnitude.

The missed event total and bin fractions for the second parameter space are plotted in Fig. 6, analogous to Fig. 3. The fact that Fig. 6a closely resembles Fig. 4a indicates that most missed events occur in the part of the parameter space containing the majority of the tornado reports. On a case-by-case basis (Fig. 6b), missed events are far less common for large values of 0-6 km vector shear magnitude and MU CAPE. A bit of a threshold is suggested, in which events are more likely to be missed for environments having less than about 20 kt of vector shear magnitude, regardless of the value of MU CAPE.

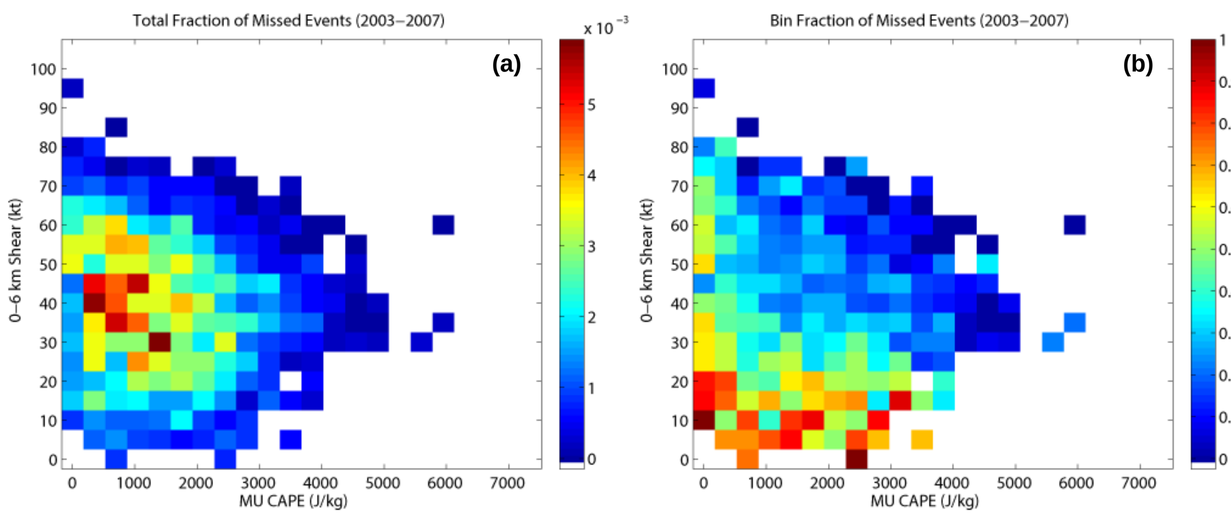

Figure 6: As in Fig. 3, but for most unstable CAPE (J/kg) and 0-6 km vector shear magnitude (kt). Each bin represents a range of the environmental parameter space, and bins containing fewer than 5 events have been removed. (a) Total fraction of missed events: note the similarity to the total number of reports in Fig. 4a. (b) Bin fraction of missed events.

3.3 Lead Times

Another important measure of tornado warning skill is that of lead time, i.e., the amount of time that elapses between a tornado warning and the associated tornado report. [See Simmons and Sutter (2008) for a more detailed description of lead time as a measure of forecast skill.] For the 7190 tornado reports considered in this study, the average lead time (counting missed events as a lead time of 0 min) was 13.59 minutes. Without including missed events, the average lead time was 19.72 minutes. Figure 7 provides a geographical perspective on these warning events, demonstrating where the majority of tornadic events occur, as well as where missed events are most common. Any trends are difficult to pick out of the thousands of plotted points, but regions with relatively few tornadoes tend to have a higher number of missed events (e.g., west of the Rocky Mountains), and certain coastal regions also tend to have more missed events (e.g., the coasts of Florida and the Gulf coast of Texas).

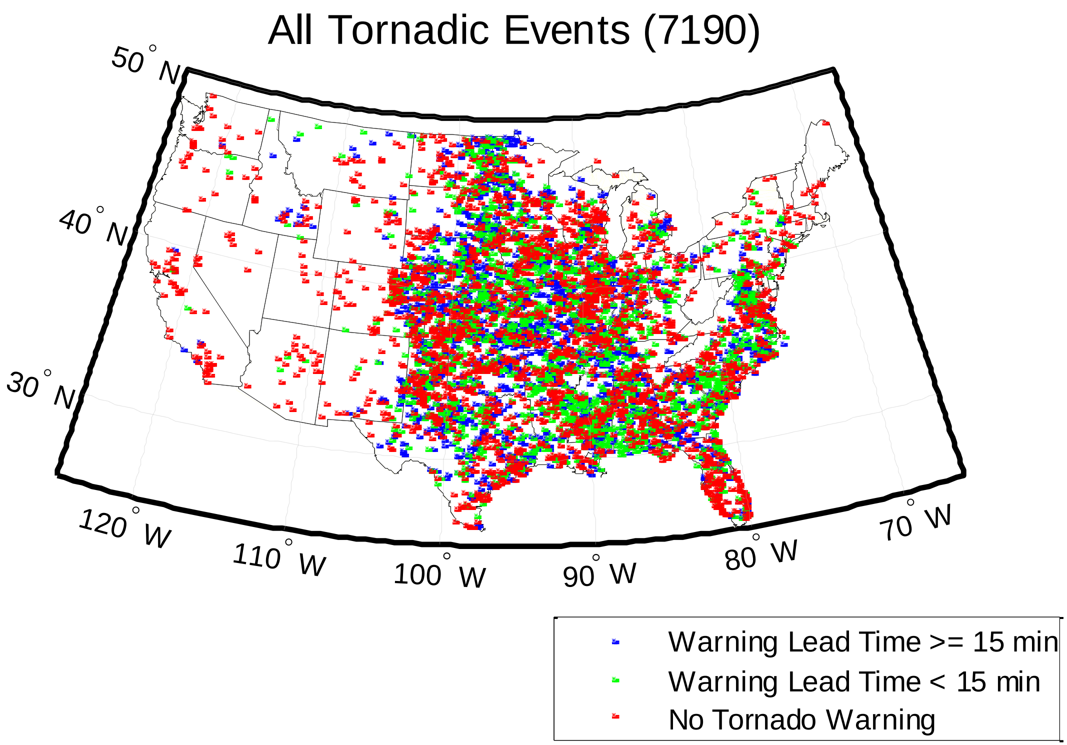

Figure 7: Geographical depiction of warning lead times for the continental United States, 2003-2007. Note that the "No Tornado Warning" category here includes warnings with lead times of zero minutes, which are sometimes counted as 'hits' in the verification literature.

In order to clarify some of the trends that may be obscured by the plethora of data in Fig. 7, Figs. 8 and 9 focus solely on strong shear events (i.e., those events having 0-6 km vector shear magnitude greater than 35 kt). Figure 8 plots only the lead times for those events having relatively low instability (ML CAPE of 100-1000 J/kg) in addition to this vector shear magnitude, while Fig. 9 shows the events with relatively high instability (ML CAPE ≥ 2000 J/kg). Table 1 summarizes the lead times for each of these categories.

Table 1: Warning lead times for all events, low instability/strong shear events, and high instability/strong shear events. See captions for Figs. 8 and 9 for further information on the stability definitions.

	Including Misses	Not Including Misses
All Events	13.59 min	19.72 min
Low Instability	12.40 min	17.89 min
High Instability	17.90 min	21.95 min

The shear requirement for both Figs. 8 and 9 clearly eliminates the majority of the events in less tornado-prone regions (i.e., west of the Great Plains). Missed events along the Florida and Gulf coasts have also largely been filtered out.

In the low-instability cases of Fig. 8, the majority of tornadoes occur in the Southeast. These events have an average warning lead time that is just over one minute less than the average for all events (including misses), or just under two minutes less than the average for all events (not including misses). The percentage of missed events is similar for the low-instability cases and for the set of all cases.

In contrast, Fig. 9 shows the high-instability events, generally centered more over the Great Plains. These events have a warning lead time that is over four minutes better than the average for all events (including misses), or just over two minutes better than the average for all events (not including misses). Consistent with this, the percentage of missed events also is lower for the high-instability/strong-shear events, as compared with either low-instability or weak-shear events. These results, and similar plots for false alarms, can provide some guidance as to whether or not operational tornado forecasting criteria and methodologies are effectively increasing warning lead times.

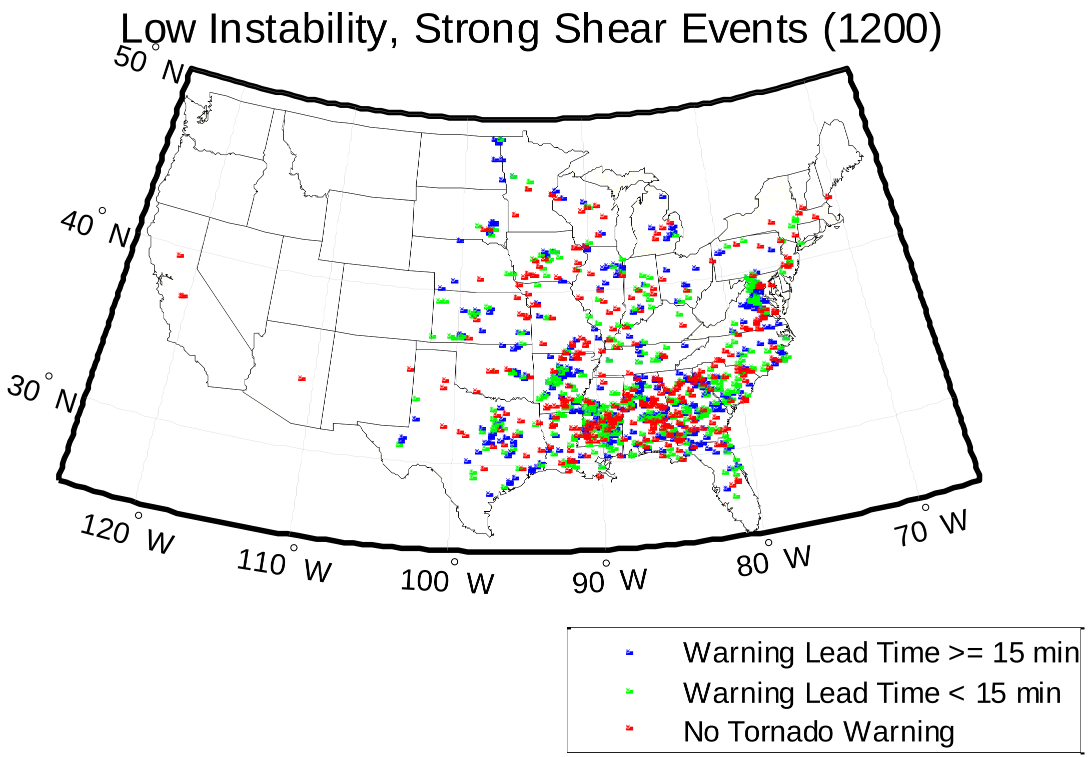

Figure 8: Geographical depiction of warning lead times for low instability, strong shear events in the continental United States, 2003-2007. These 1200 events meet the following criteria: ML CAPE 100-1000 J/kg, ML LCL < 1000 m, 0-6 km vector shear magnitude ≥ 35 kt, 0-1 km vector shear magnitude ≥ 18 kt, and ML CIN ≥ -100 J/kg.

4. FUTURE WORK

This early work is the very beginning of our investigation into warning skill. Given the wide variety of environmental parameters available, future work will include similar examinations of warning skill with respect to other combinations of environmental parameters. An examination of skill by tornado intensity will also provide guidance to determine environmental skill discriminators for weak and significant tornadoes. More broadly, we will identify the storm types contributing to various portions of the parameter space, and perform an examination of the impact of environmental heterogeneity on warning skill. Throughout these investigations, the environments having a high fraction of both misses and false alarms have been highlighted as a portion of the parameter space where our understanding is limited. Identifying these portions of the parameter space will enable future research to be targeted to the environmental conditions that will benefit most from the additional attention.

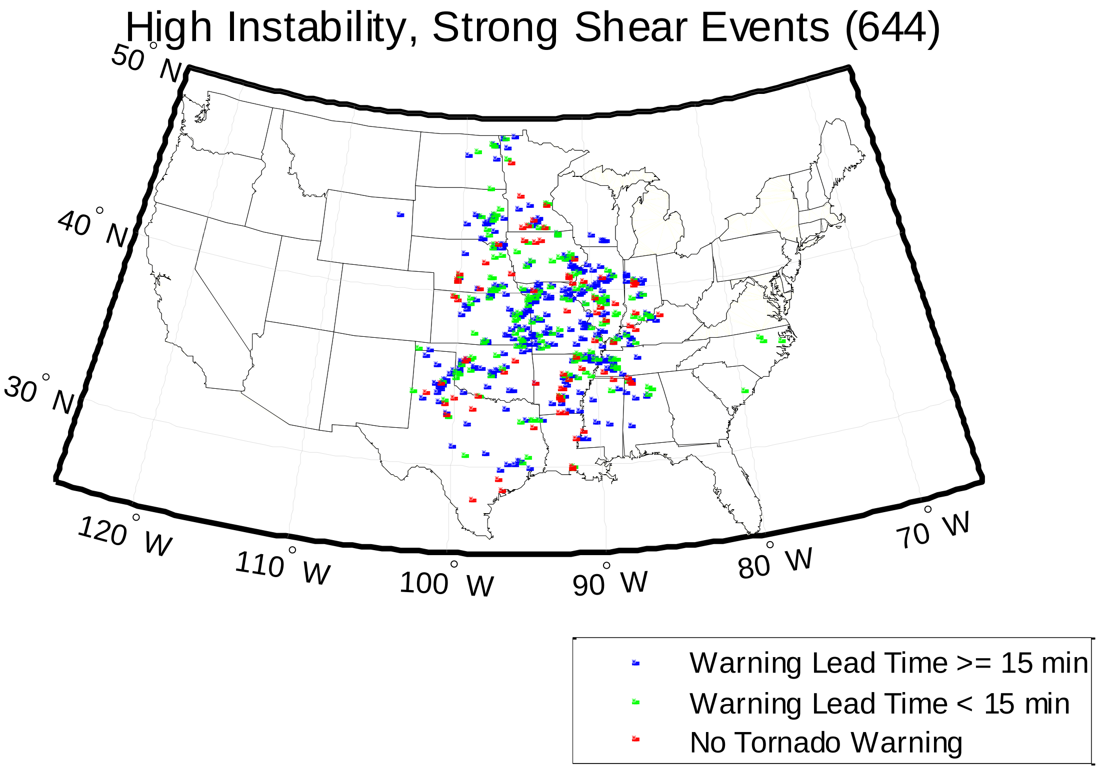

Figure 9: Geographical depiction of warning lead times for high instability, strong shear events in the continental United States, 2003-2007. These 644 events meet the following criteria: ML CAPE ≥ 2000 J/kg, 0-6 km vector shear magnitude ≥ 35 kt, and ML CIN ≥ -100 J/kg.

5. ACKNOWLEDGMENTS

The authors are grateful for the assistance from Brenton MacAloney for obtaining the verification data. This work has benefited tremendously from helpful discussions with Russ Schneider, Steven Weiss, Bill Bunting, Rich Thompson, Roger Edwards, and Paul Markowski. Alexandra Anderson-Frey is supported through a Natural Science and Engineering Research Council of Canada Fellowship.

6. REFERENCES

Bothwell, P.D., J.A. Hart, and R.L. Thompson, 2002: An integrated three dimensional objective analysis scheme in use at the Storm Prediction Center. *Preprints, 21st Conf. on Severe Local Storms*, San Antonio, TX, Amer. Meteor. Soc., J117-J120.

Brooks, H.E., J.W. Lee, and J.P. Craven, 2003: The spatial distribution of severe thunderstorm and tornado environments from global reanalysis data. *Atmos. Res.*, **67**, 73-94.

Coniglio, M.C., 2012: Verification of RUC 0-1-h forecasts and SPC mesoscale analyses using VORTEX2 soundings. *Wea. Forecasting*, **27**, 667-683.

Dean, A., and R.S. Schneider, 2008: Forecast challenges at the NWS Storm Prediction Center relating to the frequency of favorable severe storm environments. *Preprints, 24th Conf. on Severe Local Storms*, Savannah, GA, Amer. Meteor. Soc.

Markowski, P., C. Hannon, J. Frame, E. Lancaster, and A. Pietrycha, 2003: Characteristics of vertical wind profiles near supercells obtained from the Rapid Update Cycle. *Wea. Forecasting*, **18**, 1262-1272.

Rasmussen, E.N., and D.O. Blanchard, 1998: A baseline climatology of sounding-derived supercell and tornado forecast parameters. *Wea. Forecasting*, **13**, 1148-1164.

Schneider, R.S., and A.R. Dean, 2008: A comprehensive 5-year severe storm environment climatology for the continental United States. *Preprints, 24th Conf. on Severe Local Storms*, Savannah, GA, Amer. Meteor. Soc.

Simmons, K.M., and D. Sutter, 2008: Tornado warnings, lead times, and tornado casualties: An empirical investigation. *Wea. Forecasting*, **23**, 246-258.

Thompson, R.L., R. Edwards, J.A. Hart, K.L. Elmore, and P. Markowski, 2003: Close proximity soundings within supercell environments obtained from the

Rapid Update Cycle. *Wea. Forecasting*, **18**, 1243-1261.
____, B.T. Smith, J.S. Grams, A.R. Dean, and C. Broyles, 2012: Convective modes for significant severe thunderstorms in the contiguous United States. Part II: Supercell and QLCS tornado environments. *Wea. Forecasting*, **27**, 1136-1154.